Nonlinear Effect on Ship Generated Mini-tsunamis

Jinyu Yao[1]*, Xinshu Zhang[1], Robert F. Beck[2]

[1]State Key Laboratory of Ocean Engineering, Shanghai Jiao Tong University, Shanghai 200240, China

[2]Department of Naval Architecture and Marine Engineering, University of Michigan, Ann Arbor MI 48109, USA

1   Introduction

The condition of waves generated by a ship in steady motion in finite depth water varies with the ship's speed U. The depth Froude number $Fr = \frac{U}{\sqrt{gh}}$ (where g is the acceleration of gravity and h is the water depth) is widely adopted to measure the velocity. If a ship moves with a subcritical speed ($Fr < 1$) in water with a flat bottom, a wave wake and a depression along the ship are formed. The phenomenon called 'squat' happens when the depth is shallow (Tuck, 1966). Under the near-critical and supercritical conditions, nonlinear effects can not be ignored. Ertekin *et al.* (1984) found a series of solitons in the experiment when $Fr > 1$. The solitons begin to break at $Fr = 1.2$ and are replaced by a hydraulic jump at $Fr = 1.3$. Chen & Sharma (1995) used a Kadomtsev-Petviashvili equation to investigate a slender ship moving in a shallow channel. As for $Fr = 0.9$, 1.0, 1.1, they obtained similar results with Ertekin *et al.* (1984). In addition, they also considered the influence of the channel width on the amplitude of solitons and the period of the first two solitons. Wu (1987) explained the basic mechanism of the formation of upstream solitons and studied the nonlinear stability based on the forced Korteweg-de Vries equation. Li & Sclavounos (2002) investigated the three-dimensional nonlinear waves generated by a ship traveling at different speeds in an unbounded domain. The parabolic crestline of solitons is shown in shallow water and parabolic water humps are formed when $Fr > 1.2$.

Recently, different from the nonlinear solitons mentioned above, a new type of upstream wave named 'mini-tsunami' was observed in Norway (Grue, 2017). Mini-tsunamis are generated when large ships travel across a shallow depth variation with subcritical speed. These ship-induced upstream waves can cause erosion, and it is worth investigating them.

Because the amplitude and wavelength of mini-tsunamis are 2 m and 100 m, respectively, linear free-surface boundary conditions were used by Grue (2017). The ship was modelled by a moving pressure distribution. He studied the influence of channel width and the ship's velocity on the amplitude of mini-tsunamis. Later, he developed a model for a real ship geometry and explained the generation process of mini-tsunamis (Grue, 2020). The results showed that the differences between the calculations for a real ship geometry and those for a pressure distribution are not obvious.

The slope of a mini-tsunamis, which is defined as the ratio between the height and the length, is in the linear regime, so linear free-surface boundary conditions were used in two papers of Grue. However, the nonlinear effects have not been studied and the importance of nonlinearity is still unclear. With this motivation, we used a High-Order Spectral (HOS) method and a Boussinesq model, FUNWAVE-TVD, to model the nonlinear evolution of the free surface over a variable bottom. Comparing the results of the HOS model, FUNWAVE-TVD and Grue's method, we can examine the nonlinear effects in different conditions where the ship's draft and velocity are the main variables.

2   Fully nonlinear numerical models
2.1   HOS model with variable bathymetry (HOS-VB)

A potential flow formalism is used and the flow can be described by a velocity potential ϕ (Gouin *et al.*, 2017). The two horizontal axes are x and y, and the horizontal computational domain can be defined as $L_x \times L_y$. The vertical axis z points upwards and the mean water level is at $z = 0$. Based on the potential flow assumption, the governing equation is the Laplace equation: $\nabla \phi = 0$. The surface potential $\phi^S(x, y, z, t) = \phi(x, y, \eta(x, y, t), t)$ is introduced here, then the nonlinear free-surface boundary conditions are

$$\eta_t + \nabla_1 \phi^S \cdot \nabla_1 \eta - (1 + \nabla_1 \eta \cdot \nabla_1 \eta) \phi_z(x, y, \eta, t) = 0, \quad at \ z = \eta \tag{1}$$

$$\phi_t^S + g\eta + \frac{1}{2} \nabla_1 \phi^S \cdot \nabla_1 \phi^S - \frac{1}{2}(1 + \nabla_1 \eta \cdot \nabla_1 \eta) \phi_z^2(x, y, \eta, t) = -\frac{p}{\rho}, \quad at \ z = \eta \tag{2}$$

where $\nabla_1 = (\frac{\partial}{\partial x}, \frac{\partial}{\partial y})$, η is the free-surface elevation, ρ, g and p are the water density, gravitational acceleration and ship pressure distribution, respectively. The total depth $-h = -h_0 + \beta(x, y)$ where h_0 is the average bottom

---

*Presenting author

and β is the bottom variation. The bottom boundary condition reads

$$\nabla_1\phi \cdot \nabla_1\beta - \phi_z(x,y,-h_0+\beta) = 0, \quad at \; z = -h_0 + \beta. \tag{3}$$

The computational domain is periodic in the x and y directions, which can be expessed by :

$$(\phi;\eta)(x=0,y,z,t) = (\phi;\eta)(x=L_x,y,z,t), \tag{4}$$
$$(\phi;\eta)(x,y=0,z,t) = (\phi;\eta)(x=x,L_y,z,t), \tag{5}$$

If the vertical velocity on the free surface, $\phi_z(x,y,\eta)$, can be solved, the time stepping of ϕ and η can be continued based on Eqns. (1) and (2).

In order to calculate ϕ_z, we use a truncated power series to express the potential, $\phi = \sum_{m=1}^{M}\phi^{(m)}$. Then we define $\phi^{(m)} = \phi_{h_0}^{(m)} + \phi_\beta^{(m)}$, where $\phi_{h_0}^{(m)}$ satisfies the flat bottom ($z = -h_0$) boundary condition: $\frac{\partial\phi_{h_0}^{(m)}}{\partial z}(x,y,-h_0,t) = 0$, while $\phi_\beta^{(m)}$ still satisfies Eqn. (3). Therefore, $\phi_{h_0}^{(m)}$ and $\phi_\beta^{(m)}$ can be expressed as:

$$\phi_{h_0}^{(m)} = \sum_p \sum_q A_{pq}^{(m)}(t)\frac{\cosh(k_{pq}(z+h_0))}{\cosh(k_{pq}h_0)}e^{ik_{xp}x+ik_{yq}y} \tag{6}$$

$$\phi_\beta^{(m)} = \sum_p \sum_q B_{pq}^{(m)}(t)\frac{\sinh(k_{pq}z)}{\cosh(k_{pq}h_0)}e^{ik_{xp}x+ik_{yq}y}, \tag{7}$$

where $k_{xp} = p\frac{2\pi}{L_x}$, $k_{yq} = q\frac{2\pi}{L_y}$ and $k_{pq} = |(k_{xp},k_{yq})|$. Then the modal amplitudes $A_{pq}^{(m)}(t)$ and $B_{pq}^{(m)}(t)$ can be solved by a Fast Fourier Transform. More specifically, $B_{pq}^{(m)}(t)$, which is a function of $A_{pq}^{(m)}(t)$, can be computed by the following method:

We assume $\frac{\beta}{h_0} \ll 1, O(\frac{\beta}{h_0}) \equiv O(\frac{\partial\beta}{\partial x}) \equiv O(\frac{\partial\beta}{\partial y})$, then the bottom condition in Eqn. (3) can be expressed by a Taylor expansion. The Taylor series of the free surface and the variable bottom are truncated at different orders. More specifically, M for the free surface and M_b for the variable bottom. Therefore, $\phi_\beta^{(m)} = \sum_{l=1}^{M_b}\phi_\beta^{(m,l)}$. If we keep terms in Eqn. (3) at the same order, we have

$$
\begin{aligned}
\left[\frac{\partial\phi_\beta^{(m)}}{\partial z}\right]_{z=-h_0} &= \sum_{l=1}^{M_b}\left(\frac{\partial\phi_\beta^{(m,l)}}{\partial z}\right)_{z=-h_0} \\
&= \sum_{l=1}^{M_b}\frac{\partial}{\partial x}\left[\frac{\beta^l}{l!}\frac{\partial^{l-1}}{\partial z^{l-1}}\left(\frac{\partial\phi_{h_0}^{(m)}}{\partial x}\right)\right]_{z=-h_0} + \sum_{l=1}^{M_b}\frac{\partial}{\partial y}\left[\frac{\beta^l}{l!}\frac{\partial^{l-1}}{\partial z^{l-1}}\left(\frac{\partial\phi_{h_0}^{(m)}}{\partial y}\right)\right]_{z=-h_0} \\
&+ \sum_{l=1}^{M_b}\sum_{j=1}^{l-1}\frac{\partial}{\partial x}\left[\frac{\beta^j}{j!}\frac{\partial^{j-1}}{\partial z^{j-1}}\left(\frac{\partial\phi_\beta^{(m,l-j)}}{\partial x}\right)\right]_{z=-h_0} + \sum_{l=1}^{M_b}\sum_{j=1}^{l-1}\frac{\partial}{\partial y}\left[\frac{\beta^j}{j!}\frac{\partial^{j-1}}{\partial z^{j-1}}\left(\frac{\partial\phi_\beta^{(m,l-j)}}{\partial y}\right)\right]_{z=-h_0}
\end{aligned}
\tag{8}
$$

$B_{pq}^{(m)}(t)$ can be solved by Eqn. (8).

2.2 FUNWAVE-TVD

The open-source FUNWAVE-TVD solver is based on a fully nonlinear Boussineq model (Chen *et al.*, 2000). The moving pressure distributions in the FUNWAVE-TVD and HOS model are the same and defined as:

$$p(x,y,t) = \rho g T f(x,t)q(y,t). \tag{9}$$

$$f(x,t) = \begin{cases} cos^2\left[\frac{\pi(|x-x^*(t)|-\frac{1}{2}\alpha L)}{(1-\alpha L)}\right] & \frac{1}{2}\alpha L \leq |x-x^*(t)| \leq \frac{1}{2}L \\ 1 & |x-x^*(t)| \leq \frac{1}{2}\alpha L \end{cases} \tag{10}$$

$$q(y,t) = \begin{cases} cos^2\left[\frac{\pi(|y-y^*(t)|-\frac{1}{2}\beta B)}{(1-\beta B)}\right] & \frac{1}{2}\beta B \leq |y-y^*(t)| \leq \frac{1}{2}B \\ 1 & |y-y^*(t)| \leq \frac{1}{2}\beta B \end{cases} \tag{11}$$

where L, B, T are the ship's length, width and draft, respectively. The center position of the ship is (x^*, y^*). α and β are the coefficients which control the shape of the draft region in x and y directions, respectively.

3 Results and discussion

Numerical simulations are performed by the two fully nonlinear models and the linear model in Grue (2017). Following the information of Color Fantasy which is the ship documented by Grue (2017), we use a small-scale model to simulate it. The results may be as a reference for the future experiments. In all simulations, the ship's length is $L = 2$ m and its beam is $B = 0.5$ m. The steady velocity of the ship is defined as U_0, and a start-up process is imposed at the initial moment: $U = U_0\sin(t/T_0)$ for $0 \leq t \leq \frac{\pi T_0}{2}$ where $T_0 = 30\sqrt{h_1/g}$ and $h_1 = 0.3$. The computational domain is $L_x \times L_y = 307.2$ m $\times$ 2 m and the total number of nodes is $N_x \times N_y = 8192 \times 128$.
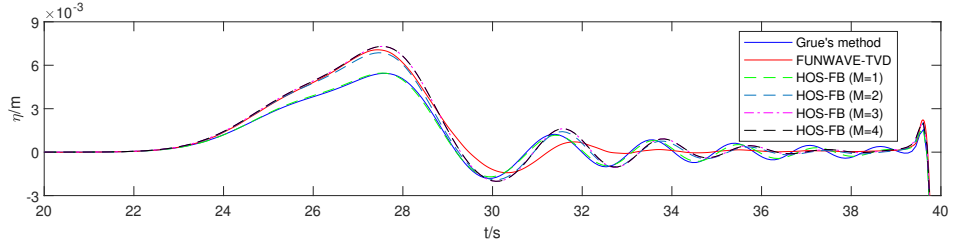
Figure 1: The upstream wave elevation induced by the start-up process on a flat bottom as recorded by the probes in different computations. $U_0 = 1.3$ m/s, $h = 0.45$ m, $Fr = U_0/\sqrt{gh} = 0.62$, $\frac{h}{T} = 4.5$.
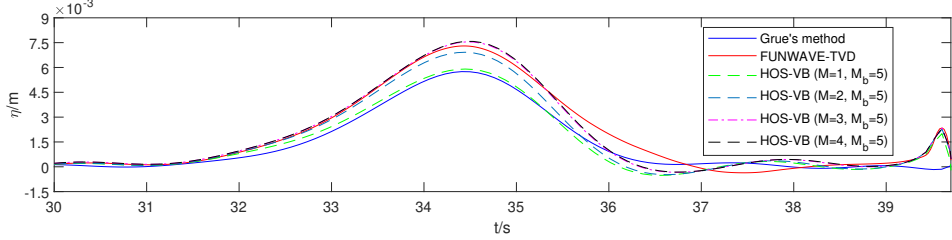

Figure 2: The upstream wave elevation induced by a variable bottom as recorded by the probes in different computations. $U_0 = 1.3$ m/s, $\Delta h = 0.75$ m, $h_0 = 0.825$ m, $Fr = U_0/\sqrt{gh_0} = 0.46$, $\frac{h_0}{T} = 8.25$.

First, we consider the influence of nonlinear effects on upstream waves induced by the ship's start-up process on a flat bottom. The velocity is $U_0 = 1.3$ m/s, the draft is $T = 0.1$ m and the depth is $h = 0.45$ m. Therefore, the non-dimensional parameter $\frac{h}{T} = 4.5$. A numerical wave probe is placed at 49.28 m in front of the initial position of ship and both of them are placed in the half-width line of the tank. The wave amplitudes at the probe that are calculated by different models are displayed in Fig. 1. As for the HOS model with flat bottom (HOS-FB), different nonlinear orders are tested, i.e. $M = 1$, 2, 3, 4. As shown in the figure, the front wave, whose peak is recorded at approximately 27.8 s, is induced by the start-up of the ship. The wave amplitudes calculated by the HOS-FB ($M = 3$) and HOS-FB ($M = 4$) are almost the same, which means that the results are converged. Although nonlinear free-surface boundary conditions are used, HOS-FB ($M = 1$) which concentrates on the first-order terms has the same wave amplitude as Grue's model. Both of them are 5.45 mm, which verifies the linear result. If the nonlinear order in HOS is set to 2, the wave peak reaches 6.86 mm. It means that the second-order nonlinearity plays an obvious role. Considering the FUNWAVE-TVD and HOS with a higher order, we find the wave amplitudes increase to approximately 7.10 mm. In order to compare the linear result and nonlinear result, and quantify the role of nonlinearity, we define a parameter $\mu = \frac{|H_{\text{HOS-VB}(M=3)} - H_{\text{Grue}}|}{H_{\text{Grue}}} \times 100\%$, then $\mu = 33.95\%$ for this flat bottom condition. To sum up, nonlinearity plays an important role in the upstream wave generated by the start-up of the ship.

Next, we investigate the nonlinear effect on the upstream waves induced by a variable bottom. The depth change $\Delta h = 0.75$ m, the average water depth $h_0 = 0.825$ m, and $\frac{h_0}{T} = 8.25$. The depth change is modeled by a function of $\beta = -\frac{1}{2}\Delta h + \frac{1}{2}\Delta h[tanh(0.35(x - x_a)) - tanh(0.35(x - x_b))]$ where the midpoints of two depth changes x_a, x_b are 128.1 m and 179.1 m, respectively. The ship starts at the position which is 25 m in front of x_a with a start-up process and two probes are placed at $x_{p1} = 152.4$ m and $x_{p2} = 174.45$ m, respectively. The case with $U_0 = 1.3$ m/s is considered first. In Fig. 2, the wave whose peak is at approximately 34.5 s is generated by the variable bottom. Comparing the calculations in HOS-VB model with different orders, we can see the wave amplitude is converged at $M = 3$. As for the linear model and low-order HOS-VB model, the results of Grue's method and HOS-VB ($M = 1$) model are almost the same. If the second-order nonlinear terms are considered, the weak peak grows to 6.92 mm. The wave amplitudes in the nonlinear models including FUNWAVE-TVD, HOS-VB ($M = 3$) are approximately 7.54 mm, which is 1.80 mm higher than those in Grue's model. Comparing the linear and high-order nonlinear results, we get $\mu = 31.13\%$ which represents an obvious nonlinear effect. Therefore, it seems that the nonlinearity can not be ignored.

In order to investigate the nonlinear effect systematically, we use different values of T and U_0 and set $T = 0.10$ m, $U_0 = 1.3$ m/s as a reference. The draft remains 0.1 m and U_0 is chosen as 1.1 m/s and 1.5 m/s,

Table 1: The values of μ in different working conditions.

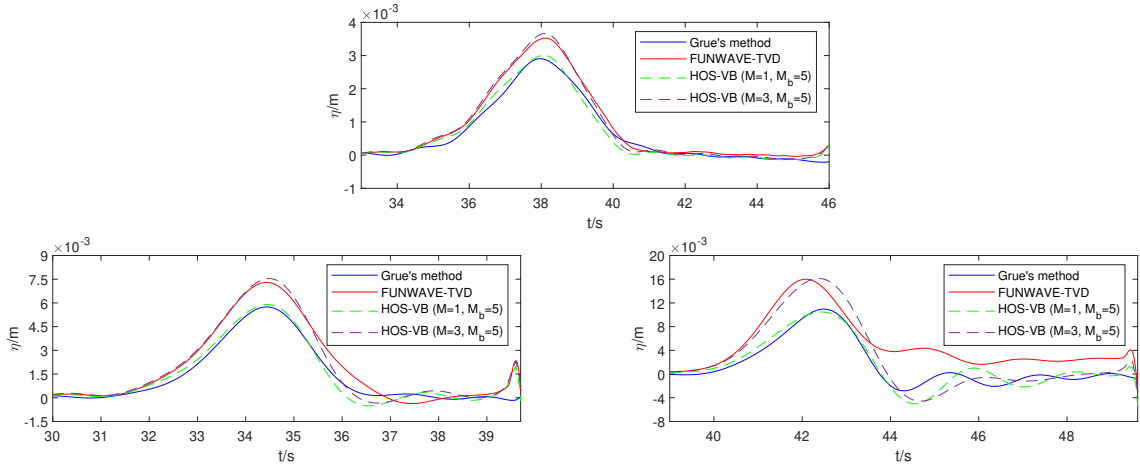| T	h_0/T	U_0	Fr	μ	U_0	Fr	T	h_0/T	μ
		1.1 m/s	0.39	26.11%			0.05 m	16.50	14.53%
0.10 m	8.25	1.3 m/s	0.46	31.13%	1.3 m/s	0.46	0.10 m	8.25	31.13%
		1.5 m/s	0.53	47.04%			0.15 m	5.50	50.81%

Figure 3: The sensitivity of the nonlinear effect on the upstream elevation to ship speed. (a) $U_0 = 1.1$ m/s, $Fr = 0.39$, the probe is placed at x_{p1}. (b) $U_0 = 1.3$ m/s, $Fr = 0.46$, the probe is placed at x_{p1}. (c) $U_0 = 1.5$ m/s, $Fr = 0.53$, the probe is placed at x_{p2}.
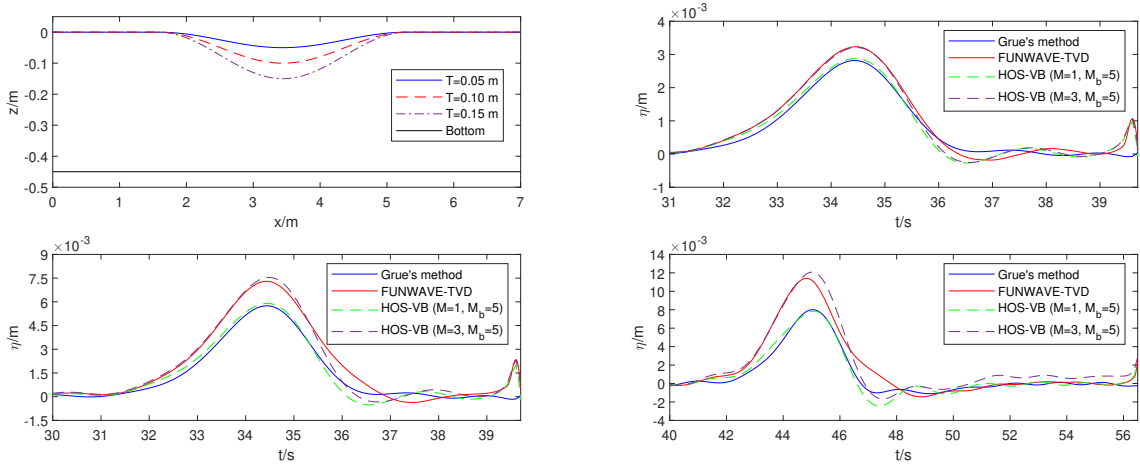

Figure 4: The sensitivity of the nonlinear effect on the upstream elevation to ship's draft. (a) Comparison of pressure distribution with different values of draft at longitudinal section in center plane with the shallow water depth. (b) $T = 0.05$ m, $\frac{h_0}{T} = 16.50$, the probe is placed at x_{p1}. (c) $T = 0.10$ m, $\frac{h_0}{T} = 8.25$, the probe is placed at x_{p1}. (d) $T = 0.15$ m, $\frac{h_0}{T} = 5.50$, the probe is placed at x_{p2}.

respectively. The Froude numbers $Fr = U_0/\sqrt{gh_0}$ of the two conditions are 0.39 and 0.53, respectively. The results with different velocities are drawn in the Fig. 3. μ in different conditions are shown in Table 1. It is evident that μ increases with the steady velocity. That means the nonlinear effect is more important when the Froude number is high. Finally, U_0 remains 1.3 m/s and the draft is chosen as 0.05 m, 0.10 m and 0.15 m. Therefore, $\frac{h_0}{T}$ of the three conditions are 16.50, 8.25 and 5.50, respectively. The results with different drafts are displayed in the Fig. 4. In Fig. 4(a) pressure distribution with different values of draft at a longitudinal section in the center plane is compared with the shallow water depth. By analyzing the value of μ in Table 1, we find the nonlinearity is more obvious in conditions with a larger draft. μ can even increase to 50.81% when the draft is 0.15 m. It can be concluded that the nonlinear effects have an influence on the upstream wave generated by the depth change and is more significant when the parameter $\frac{h_0}{T}$ is small or the depth Froude number is high.

References

CHEN, Q., KIRBY, J. T., DALRYMPLE, R. A., KENNEDY, A. B. & CHAWLA, A. 2000 Boussinesq modeling of wave transformation, breaking, and runup ii: 2d. *J. Waterw. Port. Coast. Ocean. Eng.* **126** (1), 48–56.

CHEN, X. N. & SHARMA, S. D. 1995 A slender ship moving at a near-critical speed in a shallow channel. *J. Fluid Mech.* **291** (1), 263–285.

ERTEKIN, R. C., WEBSTER, W. C. & WEHAUSEN, J. V. 1984 Ship-generated solitons. In *Proc. 15th Symp. Nav. Hydrodyn, Hamburg*.

GOUIN, M., DUCROZET, G. & FERRANT, P. 2017 Propagation of 3d nonlinear waves over an elliptical mound with a high-order spectral method. *Eur. J. Mech. B Fluids.* **63**, 9–24.

GRUE, J. 2017 Ship generated mini-tsunamis. *J. Fluid Mech.* **816**, 142–166.

GRUE, J. 2020 Mini-tsunami made by ship moving across a depth change. *J. Waterw. Port. Coast. Ocean. Eng.* **146** (5), 04020023.

LI, Y. & SCLAVOUNOS, P. D. 2002 Three-dimensional nonlinear solitary waves in shallow water generated by an advancing disturbance. *J. Fluid Mech.* **470** (1), 383–410.

TUCK, E. O. 1966 Shallow-water flows past slender bodies. *J. Fluid Mech.* **26** (1), 81–95.

WU, T. Y. 1987 Generation of upstream advancing solitons by moving disturbances. *J. Fluid Mech.* **184** (1), 75–99.